ICCBT2008

Flash flood and sediment modeling with TREX

Pierre Julien, Colorado State University, Fort Collins, CO, USA
Mark Velleux, HydroQual, Inc., Mahwah, NJ, USA
John F. England, Jr., U.S. Bureau of Reclamation, Denver, CO, USA
James Halgren, Colorado State University, Fort Collins, CO, USA

ABSTRACT

TREX is a physically-based, distributed model that simulates flash floods, sediment transport, and chemical transport and fate processes at the watershed scale. Basic processes in TREX include precipitation, interception, infiltration, surface runoff, and channel flow, erosion and deposition of upland soil and channel bed sediment, and chemical transport. TREX is readily coupled with standard GIS tools to facilitate data exploration, model set-up, and provides a visual analysis of numerical results. Model performance is demonstrated through several field applications. The detailed analysis of three field sites includes: (1) flash floods on the Arkansas River basin, CO; (2) sediment transport at Goodwin Creek, MS; and (3) chemical transport at California Gulch, CO. These field studies demonstrate the importance of the links between time-variable precipitation, surface runoff, and floodplain interactions and stream flow. In addition to the magnitude and timing of floods, these interactions also control the subsequent redistribution of sediments and associated contaminants and chemicals on the land surface when flood waters inundate flood plain areas.

Keywords: Flash flood, Soil erosion, Contaminant transport, Watershed modeling.

* Corresponding author: Prof. Pierre Y. Julien, Colorado State University, Engineering Research Center, 1320 Campus Delivery, Fort Collins, CO 80523, USA, email: Pierre@engr.colostate.edu.

1 INTRODUCTION

The prediction of flash floods is a central theme in hydrologic engineering (Swain et al. 2004). Mathematical watershed models are often used to describe or simulate floods. One main reason to use rainfall-runoff models is because we have not measured variables of interest and need a way to realistically extrapolate measurements (Beven 2001). Garbrecht and Shen (1988) showed that rainfall, overland flow, channel flow and channel network phases affect runoff, peak and timing. The representation of hillslopes and channels clearly affect travel times and hydrologic response (D'Odorico and Rignon, 2003). Saco and Kumar (2004) suggest that even on large basins it is crucial to simulate hillslope dynamics. The model used in our work incorporates these important spatially-varying physical processes.

One watershed model framework that has been coupled to geographic information system (GIS) tools and applied to numerous watersheds is TREX (Velleux et al. 2006; England et al. 2007). Developed at Colorado State University, the physically-based model TREX is derived from CASC2D (Julien et al. 1995) and CASC2D-SED (Johnson et al. 2000). It is a spatially-distributed numerical model that simulates the response of a watershed subject to rainfall precipitation or snowmelt. Model processes can vary in space and time to describe precipitation, interception, infiltration, overland and channel flow, and corresponding floodplain interaction. In addition, TREX simulates a range of transport processes for particles (soil and sediment) and chemicals as well as mass transfer and transformation processes for chemicals. Key model inputs include watershed extent, a digital elevation model (DEM), soil type, and land use. Such inputs are specified as raster maps (grids) and are directly derived from GIS sources. Other needed model inputs that can also be derived or inferred from GIS data include terrain slope and stream channel network extent from the DEM, and interception, infiltration, roughness, and erosion properties from soil type and land use. The model outputs include summaries of stream flow and sediment concentration variations over time. Model outputs are also written in a format that can be imported to a GIS for visualization and time series animation.

The numerical formulation of TREX and overviews of field study applications to three watersheds are presented. The watersheds simulated are the upper Arkansas River basin, CO, Goodwin Creek, MS, and California Gulch, CO. These applications demonstrate the model's ability to simulate watershed processes, floods, and the impact floods have on soil, sediment, and chemical transport and redistribution across the land surface, as well as the use of GIS-based tools for data analysis.

2 MODEL FORMULATION

2.1 *Hydrologic Processes*

The present version of TREX is formulated to simulate single events. The hydrologic processes in the model include precipitation, interception, infiltration, depression storage, Hortonian overland flow, dead storage, and flow in stream channels. Precipitation can be uniform or distributed in space and time. When precipitation is distributed, an inverse distance weighting (IDW) algorithm is used to interpolate rainfall values in space and linear interpolation is used to distribute values in time. Interception losses are subtracted from the gross rainfall to determine the net precipitation reaching the land surface over time. In addition to precipitation, point sources of flow can be specified to overland and channel areas.

Infiltration is simulated using the Green and Ampt (1911) relationship, which assumes a sharp wetting front exists between the infiltration zone and soil at the initial water content and that the length of the wetted zone increases as infiltration progresses. Neglecting the ponded water depth at the soil surface, the infiltration rate is computed as:

$$f = K_h\left(1 + \frac{H_c M_d}{F}\right) \qquad (1)$$

$$M_d = (1 - S_e)\theta_e \qquad (2)$$

where: f = infiltration rate [L/T], K_h = effective hydraulic conductivity [L/T], H_c = capillary pressure (suction) head at wetting front [L], θ_e = effective soil porosity = (φ-θ_r) [dimensionless], φ = total soil porosity [dimensionless], θ_r = residual soil moisture content [dimensionless], S_e = effective soil saturation [dimensionless], F = cumulative infiltration depth (distance to wetting front) [L], and M_d = soil moisture deficit [dimensionless].

Overland flow can occur when the water depth on the land surface exceeds the depression storage threshold. Overland flow is governed by mass and momentum conservation as expressed by the diffusive wave approximation of the St. Venant equations computed in two dimensions (vertically integrated) (Julien et al. 1995; Julien, 2002):

$$\frac{\partial h}{dt} + \frac{\partial q_x}{dx} + \frac{\partial q_y}{dy} = i_{net} - f + W = i_e \qquad (3)$$

$$q_x = \alpha_x h^\beta \text{ and } q_y = \alpha_y h^\beta \qquad (4)$$

$$\alpha_x = \frac{S_{fx}^{1/2}}{n} \text{ and } \alpha_y = \frac{S_{fy}^{1/2}}{n} \qquad (5)$$

$$S_{fx} = S_{0x} - \frac{\partial h}{dx} \text{ and } S_{fy} = S_{0y} - \frac{\partial h}{dy} \qquad (6)$$

where: h = surface water depth [L], q_x, q_y = unit discharge in the x- or y-direction = Q_x/B_x, Q_y/B_y [L^2/T], Q_x, Q_y = flow in the x- or y-direction [L^3/T], B_x, B_y = flow width in the x- or y-direction [L], W = added point source/sink [L/T], i_e = net (excess) precipitation rate [L/T], α_x, α_y = resistance coefficient for flow in the x- or y-direction [$L^{1/3}$/T], β = resistance exponent for turbulent flow = 5/3 [dimensionless], n = Manning roughness coefficient (SI units) [T/$L^{1/3}$], S_{fx}, S_{fy} = friction slope (energy grade line) in the x- or y-direction [dimensionless], and S_{0x}, S_{0y} = ground surface slope in the x- or y-direction [dimensionless].

Similarly, channel flow can occur when the water depth in the channel exceeds the dead storage threshold. Channel flow is also governed by mass and momentum conservation as expressed by the diffusive wave approximation of the St. Venant equation computed in one dimension along the channel in the down-gradient direction:

$$\frac{\partial A_c}{dt} + \frac{\partial Q_x}{dx} = q_l + W_c \qquad (7)$$

$$Q_x = \frac{1}{n} A_c R_h^{2/3} S_{fx}^{1/2} \qquad (8)$$

where: A_c = cross sectional area of flow [L^2], Q = total discharge [L^3/T], q_l = lateral flow into or out of the channel [L^2/T], W_c = point source/sink [L^2/T], R_h = hydraulic radius of flow = A_c/P [L], and P = wetted perimeter of flow [L]. Flow can move between the overland plane and channels as a function of water surface elevation.

2.2 *Sediment Transport Processes*

The sediment transport processes in the model are advection, erosion, and deposition, both for the overland plane and stream channel. Concentrations over time are computed using the two-dimensional advection-dispersion equation (ADE). Advection is computed from flow and concentration. Erosion and deposition rates are calculated as a function of the hydraulic properties of the flow, the physical properties of the soil/sediment such as grain size and surface characteristics such as slope. Any number of particle sizes can be simulated.

The erosion of overland soils is computed from the transport capacity of the flow using a form of the Kilinc and Richardson (1973) equation for sheet and rill erosion in bare soils, modified to reflect the influence of soil type, vegetative cover, and management practice factors (Julien, 1995):

$$q_s = 1.542 \times 10^8 q^{2.035} S_f^{1.66} KCP \qquad (9)$$

where q_s = unit total sediment discharge [kg/m·s], q = unit flow discharge [m^2/s], S_f = friction slope [m/m], K = soil erodibility factor [dimensionless], C = cropping management factor [dimensionless], P = conservation practice factor [dimensionless]. K, C, and P are parameters defined for the Universal Soil Loss Equation (Wischmeier and Smith, 1978). The erosion rate is computed from the difference between the total sediment transport capacity and the transported sediment flux. Where the transport capacity is less than the transported flux, the erosion rate is zero. The erosion flux for each particle size class is apportioned from the total erosion flux based on grain size distribution and dimensionless particle diameter.

Erosion of the channel sediment bed is computed from the transport capacity of the flow for each grain size using the Engelund and Hansen (1967) equation:

$$C_w = 0.05\left(\frac{G}{G-1}\right)\frac{VS_f}{\left[(G-1)gd_p\right]^{0.5}}\left[\frac{R_h S_f}{(G-1)d_p}\right]^{0.5} \qquad (10)$$

where C_w = sediment concentration by weight, G = particle specific gravity [dimensionless], V = flow velocity [L/T], S_f = friction slope [L/L], g = gravitational acceleration [L/T^2], d_p = particle diameter [L], and R_h = hydraulic radius [L]. The transport capacity is computed from flow and C_w for each particle size class. The erosion rate is then computed from the difference between the transport capacity and the transported flux. Where the transport capacity is less than the transported flux, the erosion rate is zero. Deposition for both the overland plane and the channel network is computed from the effective fall velocity (settling speed) of each particle type.

2.3 *Chemical Transport Processes*

The chemical transport processes in the model are chemical partitioning and phase distribution; advection, erosion, deposition, infiltration and transmission loss, and a suite of mass transfer and transformation processes (chemical reactions). All processes occur in both the overland plane and stream channel. Any number of chemicals can be simulated. Advection is computed from flow and concentration. Erosion and deposition are calculated as a function of sediment transport fluxes and phase distribution.

Chemicals often partition between dissolved, bound, and particulate phases. The phase distribution describes the fraction of the total chemical concentration that is dissolved, bound, or particulate. The partition

coefficient is defined as the ratio of chemical concentration in particulate form to the dissolved concentration. Similarly, the binding coefficient is defined as the ratio of the chemical concentration in bound form to the dissolved concentration. Assuming local equilibrium, the chemical phase distribution can be computed from the concentration of solids and the chemical partition and binding coefficients (Thomann and Mueller, 1987; Chapra, 1997):

$$f_d = \frac{1}{1 + D_{oc}\mathrm{K}_b + \sum_{n=1}^{N} m_n \mathrm{K}_{p_n}} \qquad (11)$$

$$f_b = \frac{D_{oc}\mathrm{K}_b}{1 + D_{oc}\mathrm{K}_b + \sum_{n=1}^{N} m_n \mathrm{K}_{p_n}} \qquad (12)$$

$$f_{p_n} = \frac{m_n \mathrm{K}_{p_n}}{1 + D_{oc}\mathrm{K}_b + \sum_{n=1}^{N} m_n \mathrm{K}_{p_n}} \qquad (13)$$

$$f_d + f_b + \sum_{n=1}^{N} f_{p_n} = 1 \qquad (14)$$

where: f_d = fraction of chemical in dissolved phase [dimensionless]; f_b = fraction of chemical in bound phase [dimensionless]; f_{p_n} = fraction of chemical in particulate phase associated with particle n [dimensionless]; K_b = binding coefficient [L^3/M]; K_{p_n} = partition coefficient of chemical to particle n [L^3/M]; D_{oc} = concentration of dissolved organic compounds (or other binding agents) [M/L3]; m_n = concentration of particle n [M/L^3]; and n = particle index (for each type simulated) = 1, 2, 3, etc.

3 ARKANSAS RIVER, CO

3.1 *Problem Overview*

Estimates of extreme floods and probabilities are needed for hydrologic engineering and dam safety risk analysis. Extreme flood estimates are needed for situations where reservoir inflow peak discharge is greater than maximum spillway capacity, a reservoir has large carry-over storage, and/or a reservoir has dedicated flood control space. Typical extreme flood estimates include peak flow, volume, timing, and reservoir levels. Flood hydrographs include peak, volume and timing, and integrate the drainage basin and channel response to precipitation, given some initial, variable state of moisture throughout the watershed.

To conduct risk analysis and dam safety evaluations, extreme floods and probability estimates are required (USBR, 1999; USBR, 2003). Ideal inputs for flood risk analysis are frequency distributions of peak flows, volumes, and peak reservoir stages which, for dams with potentially high loss of life, might extend to very low probabilities. For U.S. Bureau of Reclamation (USBR) dam safety risk assessments, flood estimates are needed for annual exceedance probabilities that range from 1-in-10,000 (1×10^{-4}) to 1-in-100,000,000 (1×10^{-8}). Current USBR procedures to estimate these floods and associated probabilities are described by Swain et al. (2004). The approach was to extrapolate a peak-flow frequency curve assuming a two-parameter log-normal distribution fit of the 100-year peak flow and paleoflood data as shown in Figure 1.

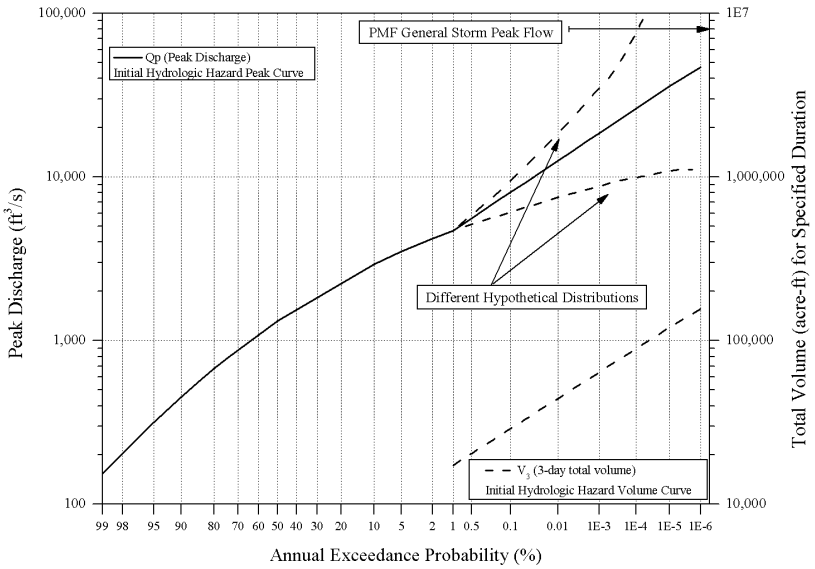

Figure 1. Example hydrologic hazard curve (after Swain et al. 2004) showing hypothetical extrapolation assumptions.

The Probable Maximum Flood (PMF) is currently recognized as a practical upper limit to flood frequency extrapolations at a site for storm durations defined by the PMF (USBR, 2002; Swain et al. 2004). One of the main problems with the current approach is the distribution assumption used for peak-flow extrapolation. The peak discharge estimate for a given probability may be substantially underestimated or overestimated; the results may potentially impact a risk analysis that uses the flood frequency information. Hypothetical examples for these situations are shown on Figure 1.

This research focused on use of a physically-based, distributed approach to derive peak-flow frequencies. Ramirez et al. (1994) suggest that the distributed approach provides a better insight of flood processes within a catchment. In contrast to widely used deterministic design procedures for large dams, such as the PMF, methods to estimate extreme floods and their probabilities are not mature (NRC, 1988) and flood frequencies are not well understood (Pielke, 1999). Burges (1998) notes that assessment of spillway adequacy for extreme floods is a major hydrometeorological issue and that critical factors include the complete spatial and temporal descriptions of extreme storms and the associated complete flood hydrograph.

3.2 *TREX Application*

The study area is the 12,000 km^2 Arkansas River basin upstream of the USBR dam near Pueblo, Colorado (Figure 2). Data for parameter estimation and calibration include: a DEM, soils, land use, streamflow (peaks, daily flows, unit values), snow depth and water equivalent at SNOTEL sites, and radar data from Pueblo and Denver. Six primary land use classes are present in the watershed based on USGS National Land Cover Data (NLCD): evergreen forest (35%), grasslands/herbaceous (29%), shrubland (23%), deciduous forest (7%), bare rock/sand/clay (3%) and pasture/hay (2%).

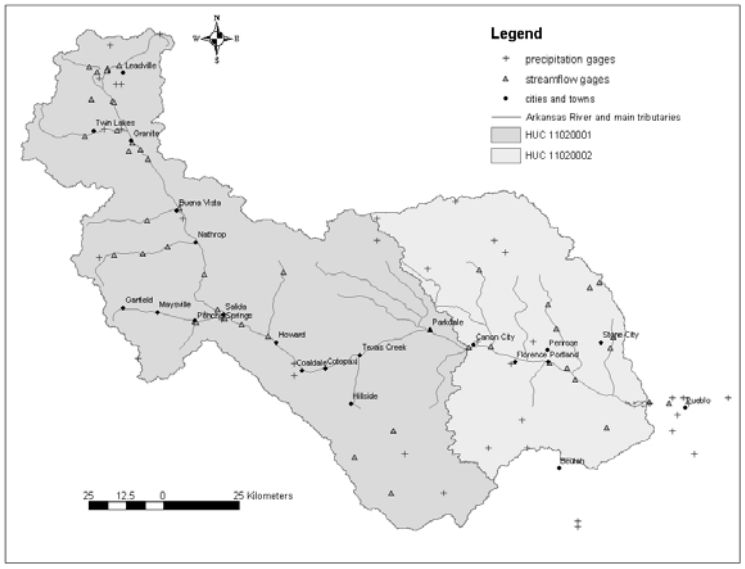

Figure 2. Arkansas River watershed upstream of Pueblo, CO.

Watershed areas with elevations greater than 3,000 m are usually snow-covered from November through mid-April. The watershed is also subject to extreme flooding in the warm season (April through August) from cloudburst rainfall, snowmelt runoff, and spring general rainstorms. Topography is the major influence on extreme precipitation. The largest recorded floods at gaging stations on the Arkansas River main stem upstream of Cañon City have been from snowmelt. At Cañon City and downstream, the largest peak flows have been from rainfall-runoff, including a disastrous June 1921 flood.

The framework to estimate flood frequency for large watersheds couples Monte-Carlo hydrologic simulations (Bocchiola et al., 2003) with a stochastic storm transposition (SST) technique (Foufoula-Georgiou, 1989; Wilson and Foufoula-Georgiou, 1990) to estimate extreme rainfall probabilities. SST is an alternative to station-based rainfall analyses. The flood frequency estimation procedure is based on the general approach outlined by NRC (1988) and the SST and runoff approach used by Franchini et al. (1996) with modifications. Spatial heterogeneities in the distribution of extreme rainfall are especially important in mountainous regions like the upper Arkansas River basin. A catalog of space-time rainfall patterns in the upper Arkansas River basin was developed from analyses of high-resolution weather radar observations (Javier et al. 2007). This "local" storm catalog for the basin was used with conventional storm catalogs of extreme rainfall to develop SST tools that reflect orographic controls of extreme rainfall. This technique was used to estimate peak flows and floods up to the Probable Maximum flood for the Arkansas River basin (England et al. 2007).

Sample results presented in Figure 3 demonstrate the importance of capturing the spatial variability of rainfall, and show excellent model calibration to the record June 1921 partial-area rain storm. The model has subsequently been used to estimate flood frequency for the Arkansas River (England et al. 2006).

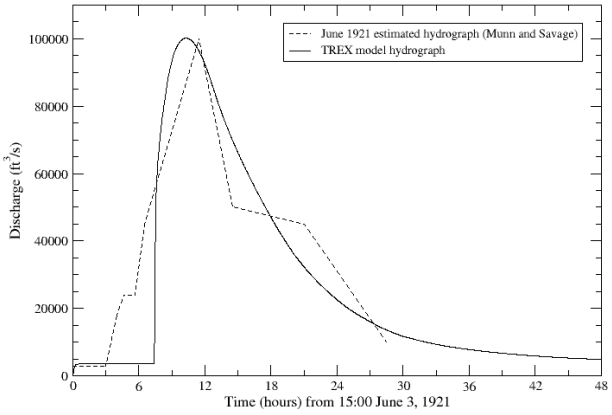

Figure 3 Hydrograph simulation for the Arkansas River.

4 GOODWIN CREEK, MS

4.1 *Site Description and Database*

Located in Mississippi, the Goodwin Creek watershed is 21.4 km^2 (Figure 4). This watershed has been extensively monitored as part of efforts to research upland erosion, instream sediment transport, and watershed hydrology (Alonso, 1996; Kuhnle and Willis, 1998). The watershed is divided into 14 nested sub-catchments with a flow-measuring flume installed at each sub-catchment outlet. The drainage areas above these gaging sites range from 1.63 to 21.3 km^2. Twenty-nine standard recording raingages are uniformly located throughout the watershed area (Blackmarr, 1995). The stream channel network and raingage locations are also shown in Figure 4.

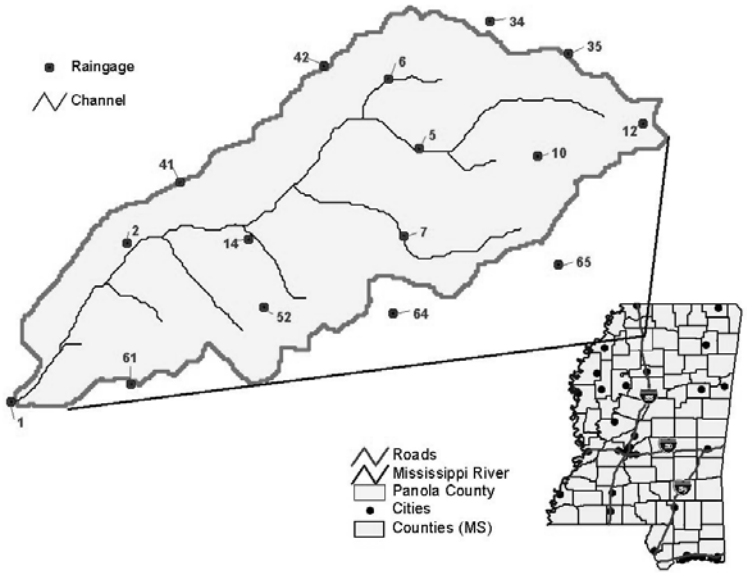

Figure 4. Goodwin Creek, MS watershed and gage locations.

Monitoring data for the watershed include runoff, sediment, and precipitation for 1981-1996. Channel cross-section data were surveyed for 1978-1988. Average annual rainfall over 1982-1992 was 1440 mm, and the mean annual runoff as measured at the watershed outlet was 145 mm/year. DEM, soil type, and land use data were obtained from the U.S. Geological Survey (USGS) and the Natural Resources Conservation Service (NRCS). Elevations in the basin range from 71 m to 128 m above mean sea level. The average slope is 0.004.

Two major soil associations are present. The Collins-Fallaya-Grenada-Calloway associations occur in terrace and floodplain locations. These soils are silty, poorly to moderately well-drained, and cover most of the cultivated area in the watershed. The Loring-Grenada-Memphis associations occur on loess ridges and hillsides. These soils are well to moderately well-drained on gently sloping to very steep surfaces and include most pasture and wooded areas in the watershed. The main types of land cover include forest, pasture, and cropland. Land use was simplified and represented as four major classifications for this study. DEM, soil type, and land use maps for the site are shown in Figure 5.

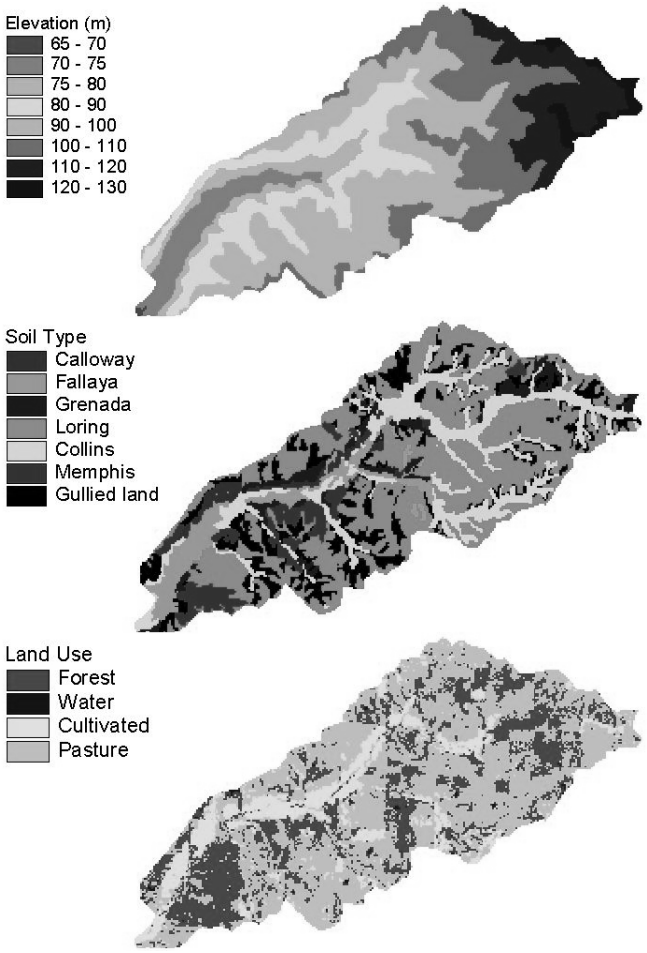

Figure 5. Goodwin Creek, MS watershed characteristics.

4.2 *Model Parameterization*

TREX was applied to the Goodwin Creek watershed. All model inputs were developed from the site database and GIS information. A storm event that occurred on October 17, 1981 was used to calibrate the model. Calibrated model parameters values are presented in Tables 1 and 2.

Table 1. Soil infiltration, erosion, and grain size distribution parameter values.

Soil Type	K_h *(cm/s)*	H_c *(cm)*	M_d	*K*	*Sand (%)*	*Silt (%)*	*Clay (%)*
Calloway	0.45	28	0.35	0.49	11	69	20
Fallaya	0.45	28	0.37	0.49	21	67	12
Grenada	0.35	20	0.35	0.49	14	72	14
Loring	0.35	28	0.32	0.49	14	73	13
Collins	0.22	20	0.35	0.43	21	68	11
Memphis	0.50	25	0.33	0.49	14	71	15
Gullied Land	0.22	15	0.38	0.24	65	27	8

Table 2. Land use, interception, roughness, and management parameter values.

Land Use	*Interception (mm)*	*Roughness (Manning n)*	*C*	*P*
Forest	3	0.25	0.002	1
Water	0	0.01	0	1
Culti-vated	1	0.15	0.090	1
Pasture	1.5	0.20	0.050	1

A model grid size of 30 m by 30 m was used. Watershed boundaries and the channel network were delineated from the DEM using a flow accumulation method. For the overland plane, interception and flow roughness (Manning n) parameters were determined from land use. For the defined land use classifications, roughness values ranged from 0.01 to 0.25 as suggested by Woolhiser (1975). Channel characteristics were developed from Blackmarr (1995) and a constant Manning n of 0.035 was used for all channel elements. Spatial distributions of infiltration parameters were derived from soil type and texture. Effective hydraulic conductivity (K_h) and capillary suction head (H_c) were developed from soil texture using the methods of Rawls et al. (1983). Soil moisture deficit (M_d) values were developed from texture-based estimates of porosity and residual moisture and the time since prior rainfall. Soil erosion properties and grain size distributions were based on the texture of the mapped soil units in the watershed. The average percentages of sand, silt, and clay as well as typical particle sizes for silty-loam soils were interpreted from the USDA (1975) texture triangle. Soil erodibility (K), cover (C), and management factors (P) were derived from the soil survey data and mapped land uses using Wischmeier and Smith (1978).

Figure 6 shows the magnitude, duration, and distribution of the precipitation data for 16 gages. Total rainfall for this event varied from 5.7 to 7.9 cm, with an average value of 7.2 cm. The event duration was 3.5 hours. Antecedent conditions were relatively dry.

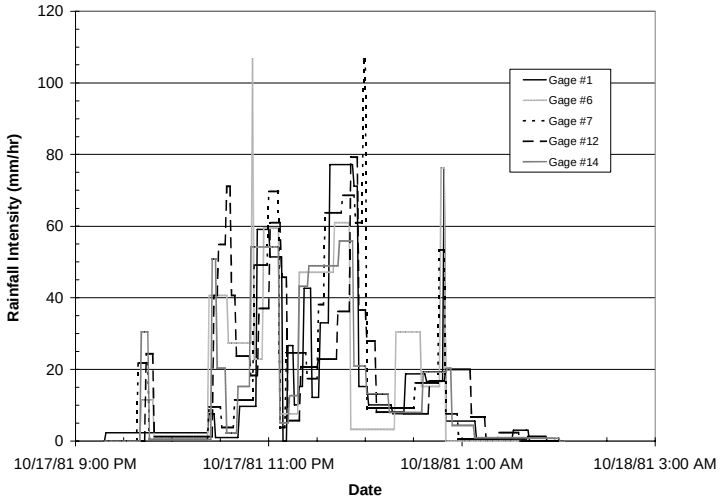

Figure 6. Goodwin Creek precipitation data at selected stations.

4.3 *Model Results*

Model performance was assessed by comparing simulation results with field measurements of surface runoff and sediment discharge at the outlet and at other locations within the basin for the October 17, 1981 event. Stream flow hydrographs and total suspended sediment concentrations for the event are presented in Figures 7 and 8.

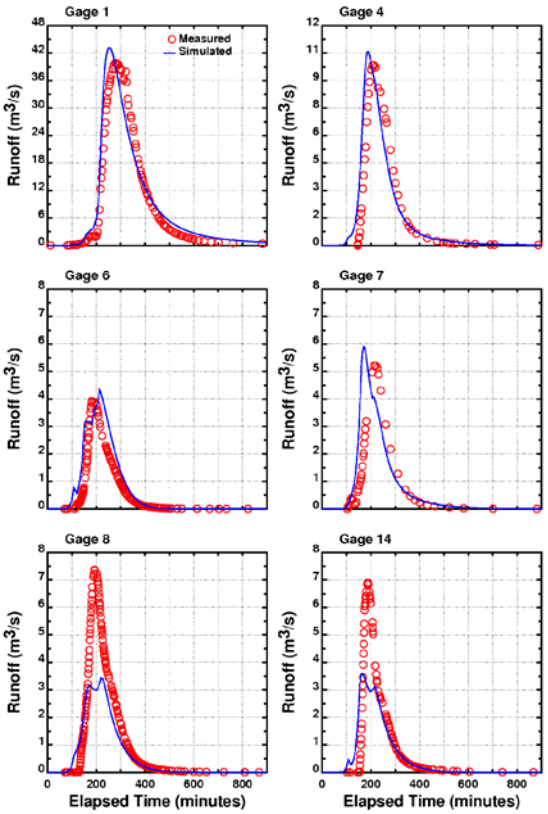

Figure 7. Observed and simulated hydrographs.

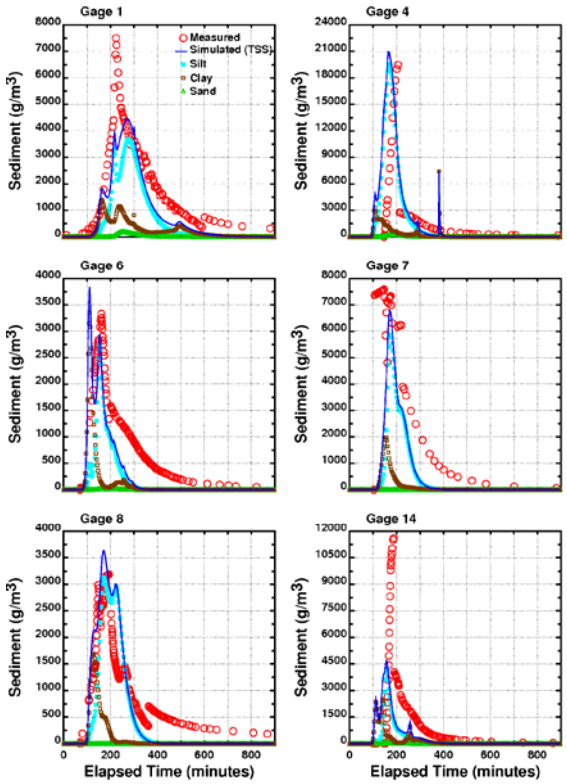

Figure 8. Observed and simulated sediment concentrations.

Regions of simulated net erosion and deposition are in agreement with field observations summarized by Johnson et al. (2000). Net erosion typically occurs in higher slope pastureland along the watershed margin and net deposition occurs in low slope valleys of the lower basin and along the main stem and tributary channels as shown in Figure 9.

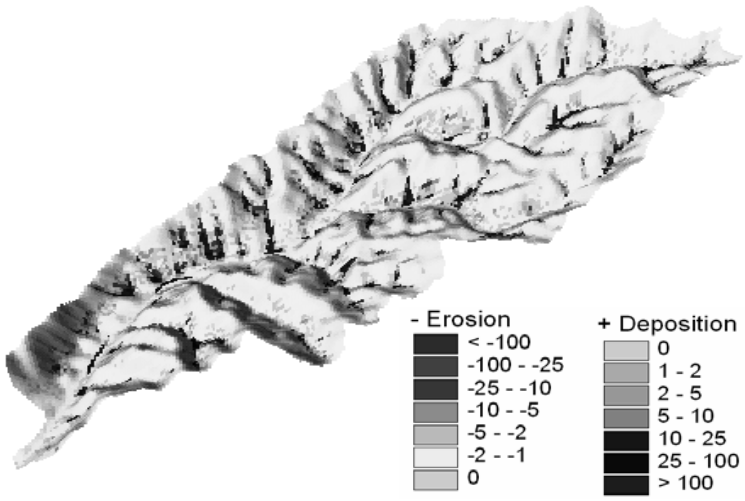

Figure 9. Simulated net erosion and deposition (mm).

5 CALIFORNIA GULCH, CO

5.1 *Site Description and Database*

California Gulch is part of a historical mining district located in central Colorado near Leadville. The site is 30.6 km^2 and lies within the headwaters of the Arkansas River watershed (Figure 10). Mining, ore milling, and smelting have occurred in the gulch since 1859 (HDR, 2002).

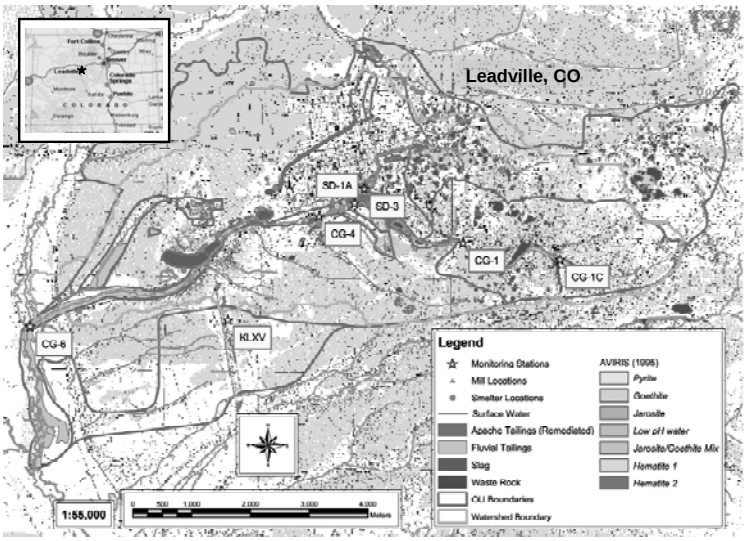

Figure 10. California Gulch (Leadville), CO watershed location, mine waste distribution, and monitoring station locations.

The watershed has been monitored as part of U.S. Environmental Protection Agency efforts to remediate the impacts of mine wastes present at the site. Monitoring data include stream flow, suspended sediment, chemical concentrations in surface water, soil, and sediment, and precipitation. Digital elevation, soils, land use, and AVIRIS remote sensing data (Swayze et al. 2000) are also available.

One legacy of mining is extensive contamination by waste rock, tailings, and slag. Approximately 2,000 waste piles are present across the site (USEPA, 1987a; WCC, 1993a-c; HDR, 2002). Environmental impacts attributable to these wastes include surface and ground water contamination from mine drainage (low pH), elevated metals concentrations on the land surface and stream channels (water column and sediment bed), and ecological impairments (toxicity to fish and benthos) (USEPA 1987a-c; Walsh, 1992; WWC, 1993a-d; Walsh, 1993; CDM, 1994). Metals of particular concern due to their toxicity to wildlife are copper (Cu), cadmium (Cd), and zinc (Zn) (Clements et al. 2002). In response to rainfall, surface erosion, and subsequent sediment transport, these contaminants are exported from the watershed and harm water quality.

The model framework for chemical transport and fate is presented in Figure 11. When simulating metals transport for single storms, volatilization, biodegradation, hydrolysis, and photodegradation can be neglected because they do not occur for the target metals or because of the short time scale for simulations. Other processes, such as dispersion and diffusion can also be neglected because at the time scale of event simulations transport processes are dominated by advection. As a result, the processes most important to simulate

metals transport are: advection; partitioning between dissolved, bound, and particulate phases; erosion and deposition of particulate chemicals, and dissolved chemical infiltration.

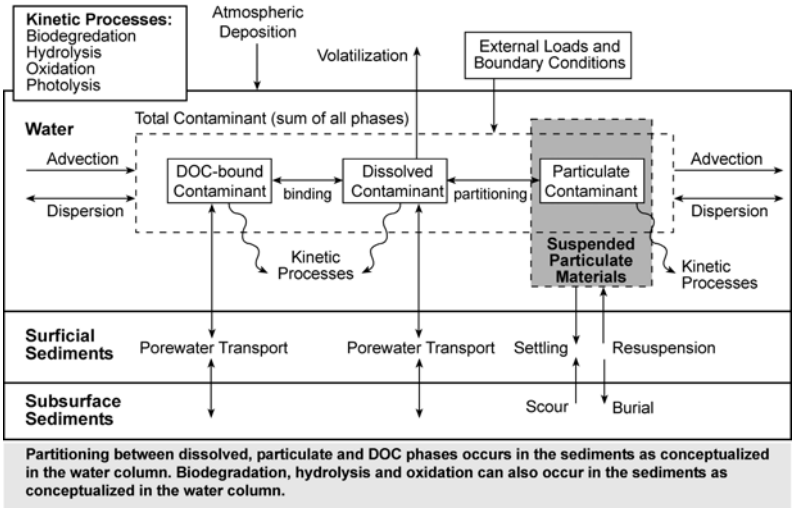

Figure 11. TREX model framework for chemical transport.

5.2 *Model Results*

The model was calibrated to two storm events (June and September, 2003) and then used to simulate system response to the 1-in-100-year, 2-hour duration storm event. Total Zn transport results at the watershed outlet for the calibration and validation events are shown in Figure 12. For the 1-in-100 year storm, low-lying parts of the watershed are subject to significant flash flooding. During this flash flood, metals are redistributed across the land surface and accumulate in flooded areas (Figure 13).

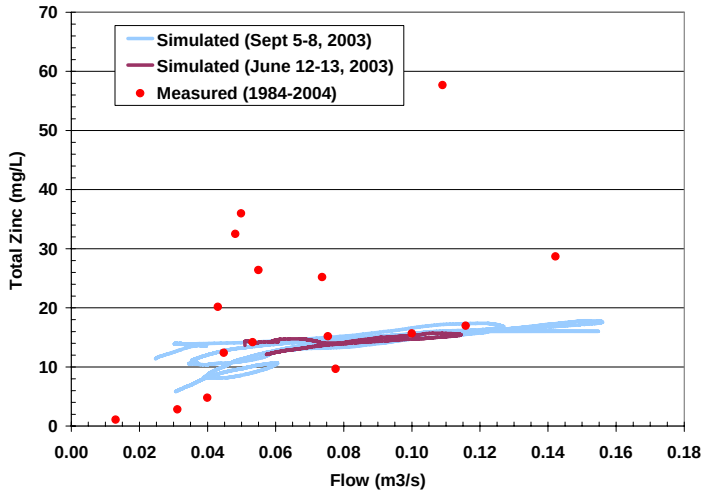

Figure 12. Simulated and Observed total Zinc concentrations vs. flow at the watershed outlet (Station CG6).

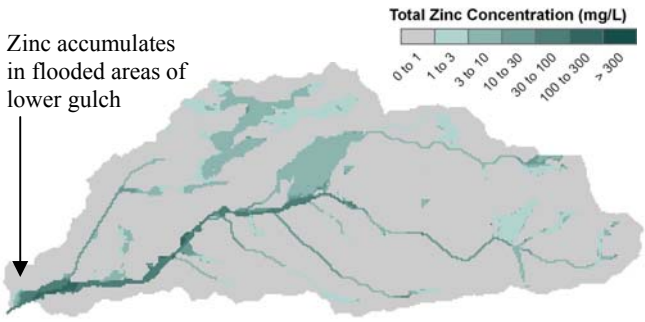

Figure 13. Simulated total zinc concentrations for the 1-in-100-year event at the end of rainfall (2 hours).

5.3 *Advanced Visualization of Flood Impact*

Modeling studies with CASC2D (Julien et al. 1995; Molnar and Julien 1998, 2000; Rojas Sánchez 2002) and TREX (Velleux 2005) have consistently used graphical output to illustrate the research results. Recent research has led to the development of improved graphical technologies to create 3-d perspective time lapse movie to provide better visualization of several surface processes including: (1) runoff from urban and forested hillslopes; (2) flow convergence and divergence from surface runoff and detention storage; and (3) flow interaction between main channel and floodplain.

A demonstration of these graphical methods is shown in Figure 14 using the 2004 application by Velleux (2005) at California Gulch near Leadville, Colorado. The 2 hour 100 yr storm distributed 1.73 inches of rain uniformly over the entire watershed. To produce the animation, grid cell values of the land surface and channel water depth were exported from the model simulation at given time intervals as raster images and these images were ingested into a GRASS GIS database (Neteler and Mitasova 2008). The maps were colorized according to the data values for each cell and then draped on a digital elevation model, also contained in the GIS. The 3-d visualization module of the GRASS systems, NVIZ, was used to produce perspective views of each of the time series and these views were assembled into an animation depicting the accumulation of runoff into distinct channels, and flood interaction between channel and floodplain. Any of the parameters tracked by the model can be incorporated into this graphical representation. Figure 14 shows a selection of frames from the hydrologic animation. Floodplain-channel interactions are especially prominent in the wetland area near the modeled watershed outlet, which is at the confluence of California Gulch with the Arkansas River.

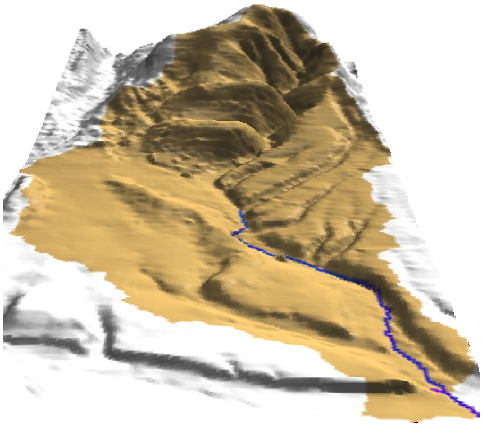

A) Pre event condition

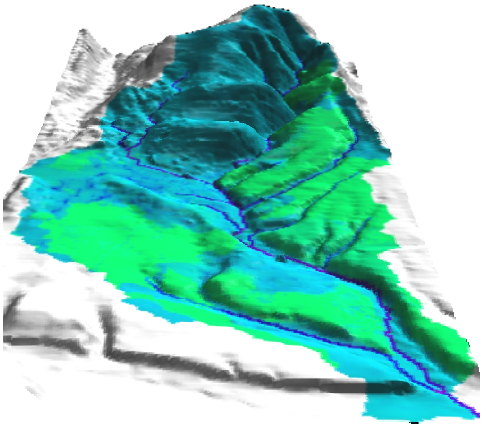

B) 30 minutes

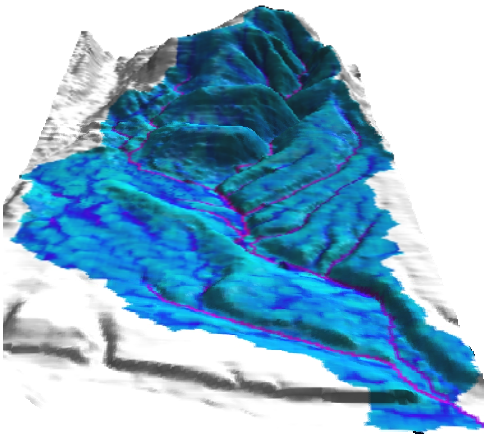

C) 2 hours (end of precipitation)

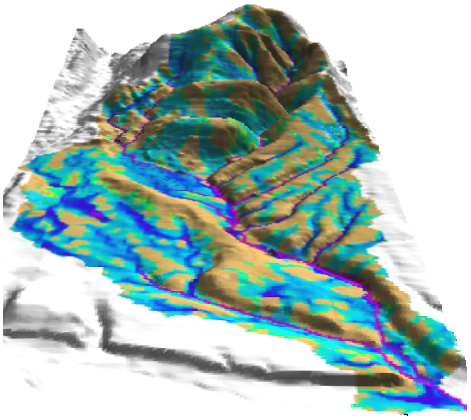

D) 3 hours

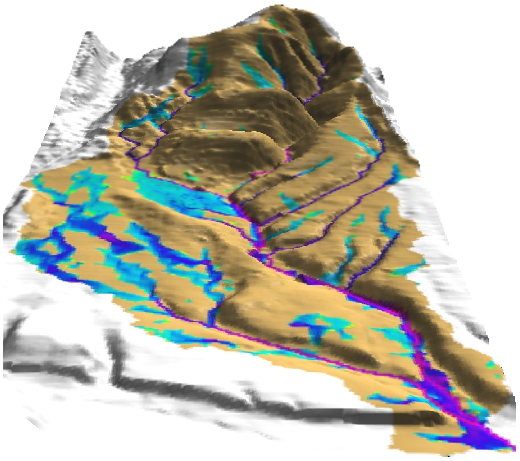

E) 4 hours

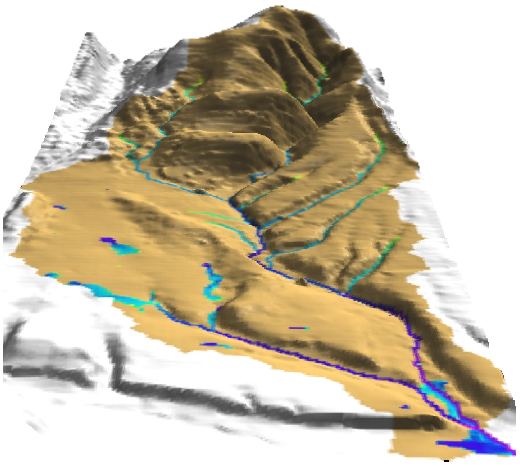

F) 12 hours

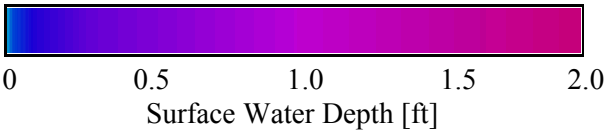

Figure 14 A -- F. Overland and channel flow depth for the 1-in-100 year even (1.73 inches in 2 hours) at California Gulch near Leadville, CO.

6 CONCLUSIONS

TREX has been applied to the Arkansas River, CO, Goodwin Creek, MS, and California Gulch, CO. For each of these field applications, the model was calibrated and validated using a variety of site-specific meteorological, stream flow, sediment, and metals concentration measurements. These field studies demonstrable model capabilities to simulate rainfall events and flash floods across a range of spatial and temporal scales. GIS was used to define model inputs and dynamically display outputs. The following conclusions can be drawn from these studies:

1. TREX correctly simulates the hydrologic response of a watershed under spatially and temporally variable rainfall for basins up to 12,000 km^2 and model resolutions from 30 to 960 m.

2. Upland erosion and deposition is successfully simulated at 30 m resolution.

3. Coupling TREX with GIS facilitates model set-up and parameterization and improves visual display of model results. Visualization of results also can help speed model calibration and verification.

4. Chemical transport can be simulated with high resolution at the watershed scale.

5. Extreme floods on large watersheds can be simulated using TREX with a derived distribution approach to estimate extreme event probabilities.

ACKNOWLEDGMENTS

Financial support was granted through the Department of Defense Center for Geosciences (DAAD19-02-2-0005 and W911NF-06-2-0015) and the Rocky Mountain Regional Hazardous Substances Research Center. Data for the Goodwin Creek application were provided by the research group of C. Alonso at the USDA-ARS National Sedimentation Laboratory in Oxford, MS. Rosalia Rojas at Colorado State University prepared initial model simulations for Goodwin Creek using CASC2D. Data for the California Gulch application were provided courtesy of S. Christensen and M. Holmes at the USEPA-Region VIII Superfund Division. We appreciate the assistance of K. King and D. Stephens at the NRMI - Colorado Mountain College in Leadville, CO. Also, collaborations with B.E. Johnson and J. Jorgeson at the U.S. Army Corps of Engineers ERDC-WES, Vicksburg, MS, and with J. D. Salas and W. Clements at Colorado State University are gratefully acknowledged.

REFERENCES

[1]. Beven, K.J., 2001. Rainfall-Runoff Modeling, The Primer. John Wiley and Sons, Chichester, 360 p.

[2]. Blackmarr, W.A. 1995. Documentation of Hydrologic, Geomorphic, and Sediment Transport Measurements on the Goodwin Creek Experimental Watershed, Northern Mississippi, for the Period 1982-1993 – Preliminary Release. Re-search Report No. 3 (CD-ROM). U.S. Department of Agriculture, Agricultural Research Service, Oxford, MS. 212 p.

[3]. Bocchiola, D., De Michele, C., and Rosso, R. 2003. Review of recent advances in index flood estimation. Hydrol. Earth Sys. Sci. 7(3):283-296.

[4]. Burges, S.J. 1998. Streamflow prediction: Capabilities, opportunities and challenges. In Hydrologic Sciences: Taking Stock and Looking Ahead, National Research Council, Washington, D.C., pp. 101-134.

[5]. CDM. 1994. Final Soils Investigation Data Report California Gulch CERCLA site Leadville, Colorado (Four Volumes). Camp, Dresser, and McKee, Inc., Denver, Colorado. Pre-pared for Resurrection Mining Company Denver, Colorado. July 15.

[6]. Chapra, S.C. 1997. Surface Water-Quality Modeling. McGraw-Hill Companies, Inc. New York, NY. 844 p.

[7]. Clements, W., Carlisle, D., Courtney, L., and Harrahy, E. 2002. Integrating observational and experimental approaches to demonstrate causation in stream biomonitoring studies. Environmental Toxicology and Chemistry, 21(6):1138-1146.

[8]. D'Odorico, P. and Rignon, R., 2003. Hillslope and channel contributions to the hydrologic response. Water Resour. Res., 39(5), 1113, pp. SWC 1-1 – SWC 1-9.

[9]. Engelund, F. and Hansen, E. 1967. A Monograph on Sediment Transport in Alluvial Stream. Teknisk Forlag 62 p.

[10]. England, J.F. Jr., Klawon, J.E., Klinger, R.E. and Bauer, T.R. 2006. Flood Hazard Study, Pueblo Dam, Colorado, Final Report. Bureau of Reclamation, Flood Hydrology Group, Denver CO, 160 p.

[11]. England, J., Velleux, N., and Julien, P. 2007. Two-dimensional simulations of extreme floods on a large watershed. Journal of Hydrology, 347(1-2):229-241.

[12]. Foufoula-Georgiou, E. 1989. A probabilistic storm transposition approach for estimating exceedance probabilities of ex-treme precipitation depths. Water Resour. Res. 25(5): 799-815.

[13]. Franchini, M., Helmlinger, K.R., Foufoula-Georgiou, E., and Todini, E. 1996. Stochastic storm transposition coupled with rainfall-runoff modeling for estimation of exceedance probabilities of design floods. J. Hydrol. (175)1-4: 511-532.

[14]. Garbrecht, J. and Shen, H.W., 1988. The physical framework of the dependence between channel flow hydrographs and drainage network morphometry. Hydrol. Process. 2, 337-355.

[15]. Green, W.H., and Ampt, G.A. 1911. Studies on soil physics – Part I: The flow of air and water through soils. Journal of Agricultural Science 4: 1-24.

[16]. HDR. 2002. Final focused feasibility study for Operable Unit 6, California Gulch NPL site, Leadville, Colorado. Report prepared for U.S. Environmental Protection Agency Region 8. HDR Engineering, Inc., Omaha, Nebraska. September 11.

[17]. Javier, J.R., Smith, J.A., England, J.F., and Baeck, M.L. 2007. The climatology of extreme rainfall and flooding from orographic thunderstorm systems in the upper Arkansas River Basin. Water Resour. Res. 43(7), 11 p.

[18]. Johnson, B.E., Julien, P.Y., Molnar, D.K. and Watson, C.C. 2000. The two-dimensional upland erosion model CASC2D-SED. J. Am. Wat. Res. Ass. 36(1): 31-42.

[19]. Julien, P.Y., 1995. Erosion and Sedimentation. Cambridge University Press, Cambridge, UK. 280 p.

[20]. Julien, P.Y. 2002. River Mechanics. Cambridge University Press, Cambridge, UK, 435 p.

[21]. Julien, P.Y., Saghafian, B., and Ogden, F.L. 1995. Raster-based hydrologic modeling of spatially-varied surface run-off. Water Resources Bulletin, AWRA 31(3): 523-536.

[22]. Kilinc, M.Y. and Richardson, E.V. 1973. Mechanics of Soil Erosion from Overland Flow Generated by Simulated Rainfall. Hydrology Papers, No. 63. Colorado State University, Fort Collins, Colorado.

[23]. Molnar, D.K., and Julien, P.Y. 1998. Estimation of Upland Erosion using GIS. Journal of Computers and Geosciences 24(2): 183-192.

[24]. Molnar, D.K., and Julien, P.Y. 2000. Grid size effects on surface runoff modeling. J. Hydrologic Engineering, ASCE 5(1): 8-16.

[25]. Neteler, M. and H. Mitasova 2008. Open source GIS: a GRASS GIS approach. New York, Springer.

[26]. NRC. 1988. Estimating probabilities of extreme floods: methods and recommended research. National Research Council, National Academy Press, Washington, D.C., 141 p.

[27]. Pielke, R.A. Jr. 1999. Nine fallacies of floods. Climatic Change 42: 413-438.

[28]. Ramirez, J.A., Salas, J.D., and Rosso, R. 1994. Determination of flood characteristics by physically-based methods. Chap-ter 6 in Coping With Floods, Rossi, G. Harmancioglu, N. and Yevjevich, V. (eds.), Kluwer Academic Publishers, Dordrecht, 77-110.

[29]. Rawls, W.J., Brakensiek, D.L., and Miller, N. 1983. Green-Ampt infiltration parameters from soils data. Journal of Hydraulic Engineering, ASCE 109(1): 62-69.

[30]. Rojas Sánchez, R. 2002. GIS-based upland erosion modeling, geovisualization and grid size effects on erosion simulations with CASC2D-SED. Colorado State University, Department of Civil Engineering. Fort Collins, Colorado.

[31]. Saco, P.M. and Kumar, P., 2004. Kinematic dispersion effects on hillslopes. Water Res. Res. 40, W01301, 12p.

[32]. Swain, R.E., England, J.F. Jr., Bullard, K.L. and Raff, D.A. 2004. Hydrologic hazard curve estimating procedures. Dam Safety Research Program Research Report DSO-04-08, U.S. Department of Interior, Bureau of Reclamation, Den-ver, Colorado, 79 p.

[33]. Swayze, G., Smith, K., Clark, R., Sutley, S., Pearson, R., Vance, J., Hageman, P., Briggs, P., Meier, A., Singleton, M., and Roth, S. 2000. Using imaging spectroscopy to map acidic mine waste. Environmental Science and Technology 34(1): 47-54.

[34]. Thomann, R.V. and J.A. Mueller. 1987. Principles of Surface Water Quality Modeling and Control. Harper and Row Publishers, Inc., New York, New York. 644 p.

[35]. USBR. 1999. Dam Safety Risk Analysis Methodology (version 3.3). U.S. Department of Interior, Bureau of Reclamation, Denver. September 1999, 48 p.

[36]. USBR. 2002. Interim Guidance for Addressing the Risk of Extreme Hydrologic Events. U.S. Department of Interior, Bureau of Reclamation, Dam Safety Off. and Technical Service Center, Denver, CO. August 19. 3p.

[37]. USBR. 2003. Guidelines for achieving public protection in dam safety decision making. U.S. Department of Interior, Bureau of Reclamation, Denver, Colorado, 19 p.

[38]. USEPA. 1987a. Phase I Remedial Investigation Report. U.S. Environmental Protection Agency, Region VIII, Denver, Colorado. May 1987.

[39]. USEPA. 1987b. Appendices: Remedial Investigation Report (Two Volumes). U.S. Environmental Protection Agency, Region VIII, Denver, Colorado. May 1987.

[40]. USEPA. 1987c. Interpretive Addenda. USEPA U.S. Environmental Protection Agency, Region VIII, Denver, Colorado.

[41]. Velleux, M. L. 2005. Spatially distributed model to assess watershed contaminant transport and fate. Colorado State University, Department of Civil Engineering. Fort Collins, Colorado.

[42]. Velleux, M.L., Julien, P.Y., Rojas-Sanchez, R., Clements, W.H., and England, J.F. 2006b. Simulation of metals transport and toxicity at a mine-impacted watershed: California Gulch, Colorado. Environmental Science and Technology, 40(22): 6996-7004.

[43]. Walsh. 1992. Soil Inventory and Map California Gulch Study Area Leadville, Colorado. Walsh and Associates, Inc., Boulder, CO. Prepared for: Glenn L. Anderson, ASARCO, Inc., Golden, CO. May 6, 1992.

[44]. Walsh. 1993. Final Smelter Remedial Investigation Report California Gulch Site Leadville, Colorado (Two Volumes). Walsh and Associates, Inc., Boulder, Colorado. Prepared for: Glenn Anderson, Environmental Manager ASARCO, Inc., Golden, CO. April 28, 1993.

[45]. WCC 1993a. Mine Waste Piles Remedial Investigation Report (Draft, Three Volumes). Woodward-Clyde Consultants, Denver, Colorado. Prepared for: ASARCO, Inc., Golden, CO, February 1993.

[46]. WCC. 1993b. Tailings Disposal Area Remedial Investigation Report (Draft, Four Volumes). Woodward-Clyde Consult-ants, Denver, Colorado. Prepared for: ASARCO, Inc., Golden, CO, February 1993.

[47]. WCC. 1993c. Surface Water Remedial Investigation Report (Draft, Three Volumes). Woodward-Clyde Consultants, Denver, Colorado. Prepared for: ASARCO, Inc., Golden, CO, February 1993.

[48]. WCC. 1993d. Aquatic Ecosystem Characterization Report (Draft). Woodward-Clyde Consultants, Denver, Colorado. Prepared for: ASARCO, Inc., Golden, CO, February 1993.

[49]. Wilson, L.L. and Foufoula-Georgiou, E. 1990. Regional rainfall frequency analysis via stochastic storm transposition. J. Hydraul. Engr., ASCE, 116(7): 859-880.

[50]. Wischmeier, W.H., and Smith, D.D. 1978. Predicting Rainfall Erosion Losses — A Guide to Conservation Planning. USDA Handbook No. 537.

[51]. Woolhiser, D.A. 1975. Simulation of Unsteady Overland Flow. In Mahmood, K., Yevjevich, V. (Eds.). Unsteady Flow in Open Channels; Vol. II; Water Resources Publications. Fort Collins, CO, p. 502.